www.rericjournal.ait.ac.th

Conversion of Cassava Rhizome to Biocrude Oil via Hydrothermal Liquefaction

Parinvadee Chukaew*,+, Kamonwat Nakason*,+,1, Sanchai Kuboon#, Wasawat Kraithong#, Bunyarit Panyapinyopol*,+, and Vorapot Kanokkantapong^,×

ARTICLE INFO

Article history:
Received 13 October 2020
Received in revised form
17 June 2021
Accepted 25 June 2021

Keywords:
Agricultural waste
Biocrude oil
Biomass utilization
Hydrothermal liquefaction
Renewable energy

ABSTRACT

Hydrothermal liquefaction (HTL) was applied to investigate the feasibility in converting cassava rhizome (CR) to biocrude oil (BO) as an alternative biofuel. HTL was performed at various process temperatures (250 – 300°C) and retention times (15 – 60 min). Process temperature is a vital key parameter on fuel properties of BO. Yield and HHV of BO were in the range of 22.90 – 31.00%, and 19.80 – 23.08 MJ/kg, respectively. The BO with maximum energy recovery efficiency (ERE) was derived at 275°C for 30 min. BO contains ketones and aldehydes, phenols, hydrocarbons, and alcohols which are in good agreement with chemical functional groups of FTIR spectra. The chemical reactions during BO formation were also proposed in this study.

1. INTRODUCTION

Biomass is the promising resource for using as fossil fuel substituting materials. It could overcome the limitations of fossil fuel uses including unsustainability and global warming. However, there are several restrictions related to the use of pristine biomass such as high moisture and volatile contents, low calorific value and bulk density, hydroscopic property, and biodegradation [1], these could reduce the biomass utilization efficiency.

Hydrothermal liquefaction (HTL) is regarded as an efficient thermochemical conversion technology that could resolve the restrictions of pristine biomass [2]. Recent years, HTL has received a huge attention for biomass utilization due to its several advantages. For example, HTL has a higher energetic efficiency than other thermochemical conversion technologies such as pyrolysis and gasification, it is normally operated at moderate temperature of 200 - 400°C [3]. HTL is also regarded as a pathogen removal process because of the operating temperature [2]. In addition, water is used as a reaction medium in HTL, it acts as both reactant and catalyst, thus wet biomass could be used resulting in no requirement of pre-drying step [4]. During HTL, water shows a dominant role because of its promising characteristics under this condition. For instance, (1) water has a low dielectric constant affected decreasing solubility of ionic molecules while increasing the solubility of hydrophobic molecules [5]; (2) viscosity of water decreases leading to enhance mass transfer and reaction rates [2]; and (3) the ionic product of water (K_w) increases resulting in water became an effective medium for acid-base catalyzed reactions without any additional catalyst [6]. Due to the water roles in HTL, biomass could be converted with the networks of chemical reactions forming biocrude oil (BO), hydrochar (HC), water soluble by-product (WSP), and syngas [3]. Biocrude oil is the desired valuable product from HTL, it can be further upgraded to value-added chemicals and transportation fuels [7], [8]. Recently, several types of biomass such as corn stover [9], eucalyptus [10], poplar wood [11], empty palm fruit bunch (EPFB) [12], birch sawdust [13], cornstalk [14], barley straw [15], and etc. were converted to BO through HTL process.

Cassava is one of the major economic crops in Thailand. In 2019, cassava was produced approximately 31 million tons [16]. Cassava rhizome (CR) is a major waste originated from cassava production. It is a part of join between cassava root and cassava stalk. Normally, CR is disposed by open burning process in the farm which leading to severe environmental pollutions especially particulate matter in ambient air. The residue product ratio of CR is 0.2 tons/ton cassava; thus the amount of CR in Thailand was approximately 6.2

*Department of Sanitary Engineering, Faculty of Public Health, Mahidol University, Bangkok, Thailand.

+Center of Excellence on Environmental Health and Toxicology (EHT), Bangkok, Thailand.

#National Nanotechnology Center (NANOTEC), National Science and Technology Development Agency (NSTDA), Pathum Thani 12120, Thailand.

^Department of Environmental Science, Faculty of Science, Chulalongkorn University, Bangkok, 10330, Thailand.

×Research Group (STAR): Waste Utilization and Ecological Risk Assessment, the Ratchadaphiseksomphot Endowment Fund, Chulalongkorn University, Bangkok 10330, Thailand

[1]Corresponding author:
Tel: +66 2 354 8540 ext 2205, Fax: +66 2 354 8540.
Email: kamonwat.nak@mahidol.ac.th.

million tons in 2019 [17]. CR is classified as lignocellulosic biomass composed mainly cellulose, hemicellulose, and lignin, these could be converted to several valuable products for replacing fossil fuel. The various research investigated the conversion of CR to several valuable products such as bio-oil [18], acetone-butanol-ethanol [19], hydrochar, and building-block chemicals [20]. However, the conversion of CR to BO through HTL has not been conducted yet.

In this study, CR was converted through HTL process at the temperature range of 250 – 300°C for 15 - 60 min. The properties of BO in terms of yield, elemental compositions, higher heating value (HHV), chemical functional group, and chemical compositions were observed. The major objective is to determine the potential of CR conversion to BO through HTL.

2. MATERIALS AND METHODS

2.1 Raw Material Preparations

CR (49.00 wt.% moisture content) was collected from Tha Muang district, Kanchanaburi province, Thailand. It was washed with tap water to remove contaminants and dried at 70°C for 24 hours. Dried CR was pulverized into powder with particles size smaller than 300 µm, and the CR powder was dried at 105°C for 24 hours. The dried CR powder was collected in sealed plastic bags for further study. The dry basis characteristics of raw CR are tabulated in Table 1.

2.2 HTL Experiments

The experiments were carried out in 120 mL stainless-steel reactor (VN Supply Co., Ltd.). The schematic diagram of HTL equipment is illustrated in Figure 1. In a typical batch experiment, 5 g dried CR powder and 50 mL distilled water were loaded in a fitting glass liner. Then, the liner was placed into the stainless-steel reactor. After that, the reactor was tightly sealed and heated in electrical furnace to desired process temperatures (250, 275, and 300°C), it was hold at each temperature for various retention times (15, 30, and 60 minutes) under stirring speed of 300 rpm. Process temperature in the reactor was observed through K–type thermocouple probe. Temperature profiles in the liquid phase are depicted in Figure A1. The retention time was recorded after the reactor was heated for 90 min to reach each process temperature.

After the retention time was completed, the reactor was suddenly placed in water bath for 30 minutes, and the product mixture was separated. The procedure of product separation is illustrated in Figure 2. Biocrude oil (BO) was extracted from solid-liquid mixture using 250 mL ethyl acetate (EA) (conc. ≥99.9%). Hydrochar (HC) was separated from the liquid by vacuum filtration through Whatman filter paper No. 2. EA soluble product (BO) was separated from water soluble product (WSP) using a separatory funnel, and its residual water was removed by anhydrous magnesium sulfate. BO was recovered from EA using a rotary evaporator. The experiments were conducted in duplication, and the third was conducted in case of inconsistency. In this article, the product samples are denoted as "PTTTt" where PT represents product types including biocrude oil (BO) and hydrochar (HC)), TT represents process temperature (250ºC (25), 275ºC (27), and 300ºC (30)), and t represents retention time (15 min (1), 30 min (3), and 60 min (6)). For example, BO273 stands for the biocrude oil sample obtained from HTL at 275ºC for 30 min.

Table 1. Raw CR characteristics.

Proximate analysis (wt.%, dry basis)		Ultimate analysis (wt.%, dry basis)	
Ash	8.32	C	39.88
Volatile matter	75.90	H	5.39
Fixed carbon	15.78	N	0.80
		S	0.47
		HHV (MJ/kg)	15.47

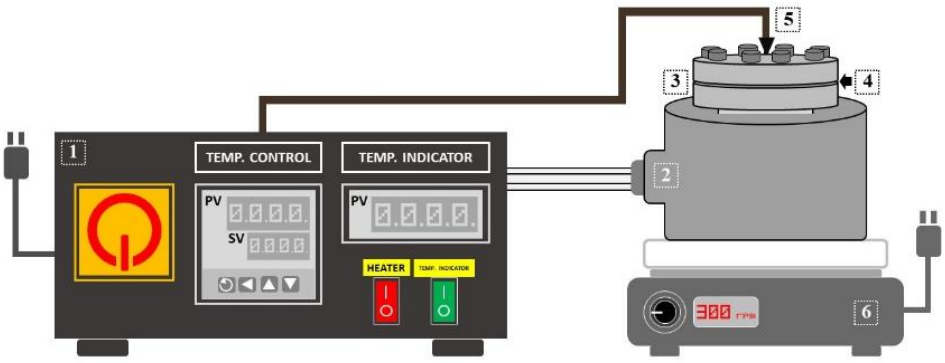

Fig. 1. Schematic diagram of HTL equipment: 1. electrical furnace controller, 2. electrical furnace, 3. stainless-steel reactor, 4. O-ring, 5. K–type thermocouple probe, and 6. hotplate stirrer.

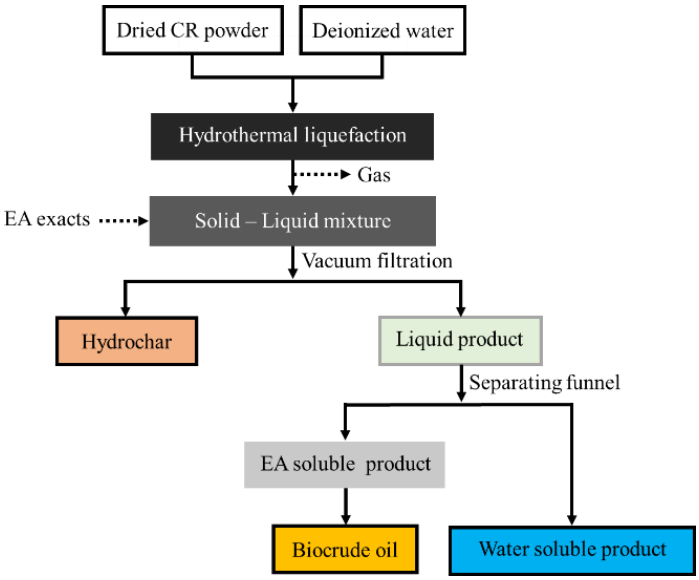

Fig. 2. The procedure of HTL process.

2.3 Characterization and Analysis

The contents of elemental compositions (CHNS) in dried CR powder and BO samples were identified using elemental analyzer (LECO CHNS 628, USA). Oxygen (O) content of each sample was calculated by deducting 100% from C, H, N, S and ash contents. Ash content was measured following the online standard analysis of NREL (NREL/TP-510-42622) [21]. Moisture and volatile matter (VM) contents in raw CR were identified according to the standard methods of ASTM D 2974-87 and ASTM D 7582, respectively [22], [23]. Fixed carbon (FC) content was determined by subtracting 100% from ash and VM contents. The chemical functional groups of dried CR powder and BO were provided using Fourier-transform infrared spectroscopy (FTIR, Thermo Scientific Nicolet 6700, USA) at infrared spectra wave number of 4000-600 cm^{-1} based on the attenuated total reflectance (ATR) method. Chemical compositions of BO were analyzed using gas chromatography – mass spectrometry (GC-MS, GC 7890A/MS5975C, Agilent technologies, USA) equipped with HP-5MS column (30 m × 0.25 mm × 0.25 µm). GC-MS was operated with the following condition: hold at 40 ºC for 4 min, ramp at 10 ºC/min to 280 ºC, and hold at 280 ºC for 20 min and the injector split ratio set to 30:1. Chemical compounds were identified using the NIST library.

2.4 Calculations

Yield (based on dried raw CS) of BO, HC, and gas and other products are calculated through Equations (1) – (3), respectively.

$$\text{BO yield (wt.\%, dry basis)} = (\text{BO mass (g)} / \text{dried raw CR mass (g)}) \times 100\% \quad (1)$$

$$\text{HC yield (wt.\%, dry basis)} = (\text{HC mass (g)} / \text{dried raw CR mass (g)}) \times 100\% \quad (2)$$

$$\text{Gas and the other products yield (wt.\%, dry basis)} = 100 - (\text{BO yield} + \text{HC yield}) \quad (3)$$

Higher heating value (HHV) of dried CR powder and BO are calculated using Dulong's formula (Equation (4)). This formula is a unified correlation of elemental contents for computation of HHV of solid, liquid, and gaseous fuels, and it is versatile because of its low average absolute error (1.45%) and bias error (0.00%) [24]. Energy density (ED) and energy recovery efficiency (ERE), and HHV improvement (HHVi) of BO are calculated using Equations (5) – (7), respectively.

$$\text{HHV (MJ/kg)} = 0.3491C + 1.1783H + 0.1005S - 0.1034O - 0.0151N - 0.021A \quad (4)$$

where C, H, S, O, N, and A represent the percentages of carbon, hydrogen, sulfur, oxygen, nitrogen, and ash, respectively.

$$\text{ED} = \text{BO HHV} / \text{Raw CR HHV} \quad (5)$$

$$\text{ERE (wt.\%)} = (\text{BO HHV} / \text{Raw CR HHV}) \times \text{BO yield} \quad (6)$$

$$HHV_i = (\text{BO HHV} - \text{Raw CR HHV}) / \text{Raw CR HHV} \quad (7)$$

3. RESULTS AND DISCUSSION

3.1 Yields of BO

Product yield is the primarily important parameter used to determine the potential of CR conversion to BO through HTL. It determines mass portion of CR feedstock contained in the resulting product after HTL. BO yield from HTL of CR at various process temperatures (250 - 300°C) and retention times (15 – 60 min) is illustrated in Figure 3. BO yield was observed to increase substantially from 24.90 to 31.00%, 24.40 to 28.60%, and 22.90 to 28.30% with increasing process temperature from 250 to 275°C at 15, 30, and 60 min, respectively, and it diminished to 27.30, 25.10, and 25.00% with further increasing temperature to 300°C. However, varying retention time affected marginally on BO yield. The maximum BO yield (31.00%) and BO/HC ratio (0.94) could be obtained from HTL at

275°C for 15 minutes. Increasing process temperature results in an increase in ionic product of water (K_w) until its maximum at 300°C, and later decreases [2]. Subcritical water is a promising medium for acid- and base-catalyzed reactions. It is accepted that biomass could be converted to BO via hydrolysis, isomerization, defragmentation, depolymerization, and condensation reactions under subcritical water [25]. Therefore, decreasing HC yield while increasing BO yield (Table A1) was due to CR compositions were decomposed through hydrolysis and deoxygenation reactions forming smaller and dissolvable products, then the products were further transformed through repolymerization and cracking reactions to form BO [26]. On the other hand, decreasing BO and HC yield simultaneously could be attributed to secondary cracking of BO, which corresponded to an increase in gas and other products [25], [27].

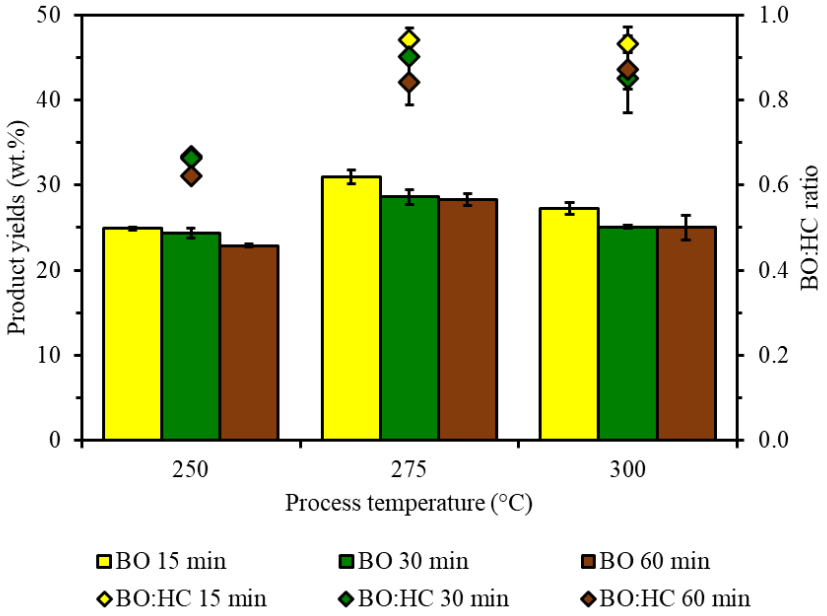

Fig. 3. BO yield and BO:HC ratio from HTL of CR at 250 – 300°C for 15 – 60 min.

3.2 Elemental Compositions and Energy Related Indexes of BO

Elemental compositions and energy related indexes of BO from HTL of CR at 250 - 300°C for 15 - 60 min are tabulated in Table 2. In comparison, carbon content in BO was much higher than that in raw CR, and it also increased with HTL temperature. In contrast, oxygen content in BO was much lower than that in raw CR, and it also decreased with the temperature. However, retention time affected only marginally in carbon and oxygen contents. Increasing carbon and decreasing oxygen contents are associated with the deoxygenation reactions [28]. These phenomena lead to much higher HHV of BO than that of raw CR, and the value also increased with increasing process temperature. Sulfur content of BO was not determined in the present study because of its very low content (0.47%) in initial CR. Additionally, ash content in BO was assumed as ash free [15], [28]. The consistent result trends were reported earlier in HTL of spent coffee ground [28], and animal carcass [25]. In comparison of an elemental composition, BO has much lower carbon and hydrogen contents than those of crude oil (83 – 87% carbon and 10 – 14% hydrogen contents), while its oxygen content is much higher than that of crude oil (0.05 – 1.5% oxygen content) [29]. Thus, the further process is required for upgrading the BO to be used as crude oil.

HHV improvement (HHVi) is used to determine the enhanced product HHV after HTL, and energy densification (ED) is used to determine the density of product energy content [30]. These values of BO increased with process temperature, the highest HHVi and ED of BO (0.49 and 1.49) were obtained from HTL at 300°C for 30 min. Energy recovery efficiency (ERE) determines the amount of feedstock energy remain within the product after HTL, it is calculated using product yield and ED [30]. Table 2 illustrates that ERE of BO varies with process condition. The highest ERE of BO (42.04%) could be obtained from HTL at 275°C for 30 minutes. However, 275°C for 15 min is suggested as the promising HTL of CR because of its short retention time with comparative BO ERE (39.55%). Similar trends of HHVi, ED, and ERE were observed in HTL of oil palm fronds [26], and microalgae [31].

3.3 Chemical Functional Groups of BO

FTIR spectra of BO from HTL of CR at 250 – 300ºC for 15 min are illustrated in Figure 4. It can be observed that the spectra of raw CR powder and BO were noticeably different. The broad transmittance peak from 3600 to 3200 cm^{-1} was ascribed to the stretching vibration of hydroxyl (-OH) and carbonyl (C=O) groups, which attribute to the present of alcoholic, phenolic, and their derivative compounds. In comparison, the intensity of this peak in BO was lower than that in raw CR. This phenomenon related with the reduction of H/C and O/C atomic ratios, and an HHV improvement. The peak at 3000 to 2800 cm^{-1} was assigned to the stretching

vibration of aliphatic and aromatic structures (C-H) [27]. This implied that BO contained more chemical compounds of both C-H aliphatic and aromatic structures. The band around 1710 and 1510 cm^{-1} was attributed to the stretching vibration of carboxyl and ester carbonyl groups (C=O), which implying to the present of carboxylic acid and ester groups [27], [28]. In BO product, the intensities of these peaks were higher than those in raw CR. The present peak at 1610 cm^{-1} was due to the present of aromatic lignin subunit (C=O) [32], which disappear in BO product. The bands at 1370 and 1240 cm^{-1} were ascribed to C–O stretching vibration in syringy and guaiacol rings, respectively [33]. The intensity of these bands in BO was higher than those in raw CR implying that BO contained both syringol and guaiacol compounds. The apparent bands at 1160 cm^{-1} presented because of the C-H deformations in plane of guaiacyl and syringyl units [33], it became more intense in BO product. The peak at 1040 cm^{-1} was due to C-O, C=C and C-C-O stretching vibration of cellulose, hemicellulose, and lignin [32]. The intensity of this peak in BO was lower than that in raw CR indicating the present of CR degradation during HTL. The peak at 757 cm^{-1} was due to out of plane C–H bending in aromatic ring structure [9], which presented obviously in BO product.

Table 2. Elemental compositions and energy related indexes of BO.

Sample name	Element analysis (wt.%)				Atomic ratio		HHV (MJ/kg)	HHV_i	ED	ERE (wt.%)
	C	H	N	O	H/C	O/C				
BO251	49.73	6.25	0.69	43.33	1.51	0.65	20.23	0.31	1.31	32.57
BO253	49.88	6.12	0.77	43.23	1.47	0.65	20.14	0.31	1.30	31.77
BO256	51.61	5.69	0.75	41.96	1.32	0.61	20.37	0.32	1.32	30.15
BO271	49.64	5.93	0.91	43.53	1.43	0.66	19.80	0.28	1.28	39.55
BO273	54.89	6.39	0.82	37.91	1.40	0.52	22.76	0.47	1.47	42.04
BO276	52.49	6.36	0.77	40.38	1.46	0.58	21.63	0.40	1.40	39.55
BO301	55.54	5.86	0.65	37.95	1.27	0.51	22.36	0.45	1.45	39.43
BO303	54.95	6.64	0.56	37.85	1.45	0.52	23.08	0.49	1.49	37.46
BO306	51.98	6.87	0.53	40.63	1.59	0.59	22.03	0.42	1.42	35.65

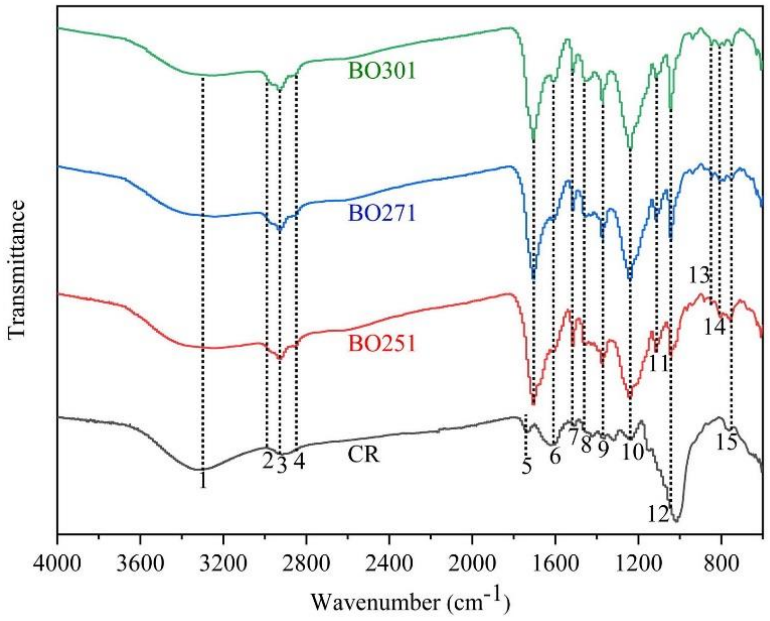

Fig. 4. FTIR spectra of BO from HTL of CR at 250 – 300 ºC for 15 minutes.

3.4 Chemical Compositions of BO

The obtained BO from HTL of CR was appeared as dark-viscous liquid, comprising the hemicellulose, cellulose, and lignin degradation products. To determine the specific chemical in BO from different HTL temperatures, the chemical compositions of BO were analyzed through GC-MS. The peak area percentage of the chemical compositions in BO from HTL of CR at 250 – 300°C for 15 min are tabulated in Table A2. The area (%) of each compound could be determined as the semi-quantitative fraction of each composition to the total peak areas. For the promising discussion, the

chemical compositions in Table A2 were classified into six categories corresponding with their functional groups including ketones and aldehydes, phenols, alcohols, hydrocarbons (aliphatics and aromatics), esters, and organic acids as illustrated in Figure 5. BO contained the chemical composition with carbon numbers varied from 5 to 32 (C5 – C32), and molecular weight range of 96.02 – 450.52. The primary chemical compositions in BO were ketones and aldehydes, phenols, and hydrocarbons, corresponding with the chemical functional groups in FTIR spectra. The maximum content of ketones and aldehydes (47.29%) in BO was obtained from HTL of CR at 300°C, while the maximum phenols (29.05%) and hydrocarbons (31.52%) contents were obtained from HTL of CR at 275°C. Interestingly, phenols and hydrocarbons could be used as an alternative source for petroleum-based chemicals and fossil fuels. The highest selectivity of phenol and hydrocarbon could be obtained at 275°C. However, at 300°C, the hydrocarbon selectivity was decreased, as the phenol selectivity was nearly stable. Ketones and aldehydes are generally originated from the conversion of monosaccharaides in cellulose and hemicellulose through hydrolysis and dehydration [34], [35], and phenol resulted from hydrolysis reaction of lignin [35], [36]. Hydrocarbons are resulted from repolymerization reaction of the primary degradation products [37]. These results determined that the chemical reactions in HTL process are the continual competitive reactions of hydrolysis, dehydration, decarboxylation, repolymerization reactions as summarized in Figure 6. In addition, there are some compounds decomposed to gaseous products at high temperature, affecting to decrease in the content of chemical compositions at 300°C.

4. CONCLUSIONS

Hydrothermal liquefaction (HTL) of cassava rhizome (CR) was conducted by varying process temperature (250 – 300°C) and retention time (15 – 60 min). The characterization of BO illustrated that process temperature played a vital role in the characteristics of BO. HTL of CR at 275°C for 30 min produced the BO with maximum ERE (42.04%). GC-MS analysis results identified that BO contained mainly ketones and aldehydes, phenols, hydrocarbons, and alcohols. The maximum phenols (29.05%) and hydrocarbons (31.52%) contents were derived at 275°C. This study determined that BO from CR could be used as alternative source for petroleum-based chemicals and fossil fuels. In addition, fractionation of chemical compositions of the BO could yield versatile organic compounds which could be further employed in various applications.

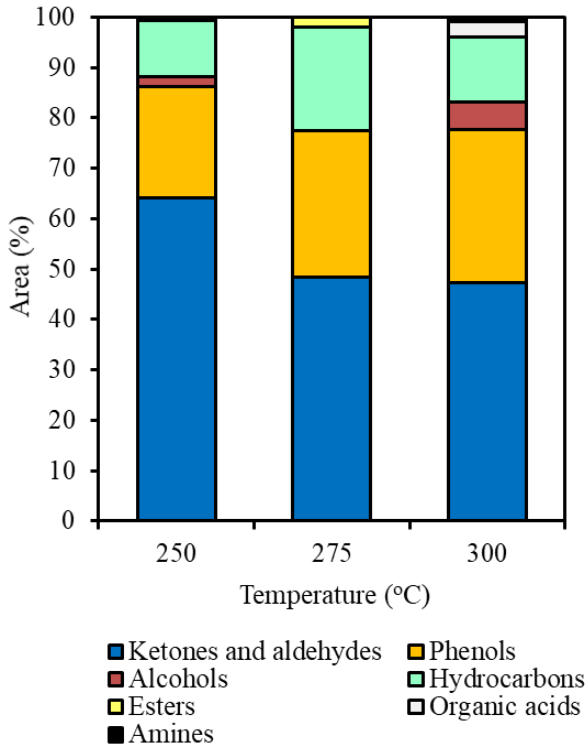

Fig. 5. Chemical compositions of BO from HTL of CR at 250 - 300 °C for 15 min identified by GC-MS.

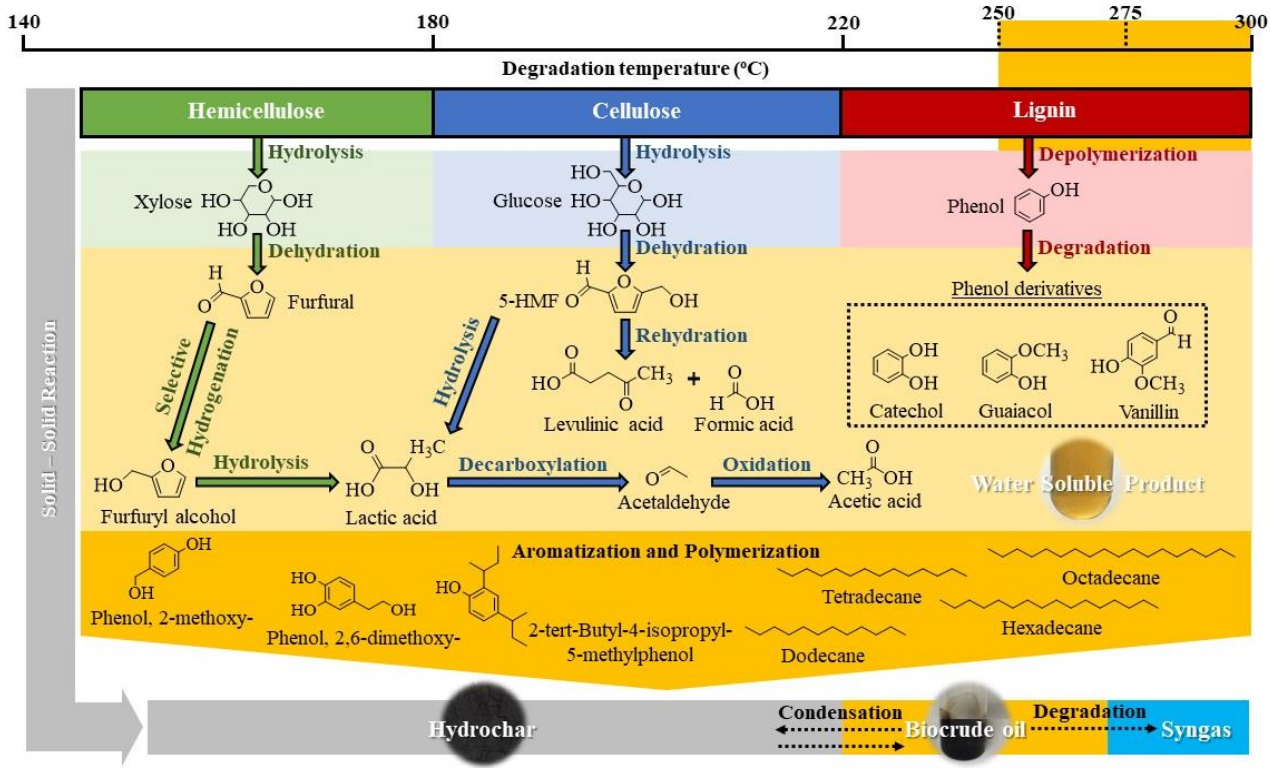

Fig. 6. The proposed chemical reactions during HTL of CR.

ACKNOWLEDGEMENT

This work is supported by the 60th Year Supreme Reign of his Majesty King Bhumibol Adulyadej Scholarship, granted by the Faculty of Graduated Studies Academic Year 2018, Mahidol University and Funding from Program Management Unit on Competitiveness (Project no. 1525064). This work is supported for publication by the China Medical Board (CMB), Faculty of Public Health, Mahidol University, Bangkok, Thailand. Financial assistance for this research was also providing by the Center of Excellent on Environmental health and Toxicology (EHT), Bangkok, Thailand.

REFERENCES

[1] Basu P., 2018. Chapter 3 - Biomass Characteristics. In P. Basu, ed. *Biomass Gasification, Pyrolysis and Torrefaction (Third Edition)*. Massachusetts: Academic Press, pp. 49-91.

[2] Singh R., Prakash A., Balagurumurthy B. and Bhaskar T., 2015. Chapter 10 - Hydrothermal Liquefaction of Biomass. In A. Pandey, T. Bhaskar, M. Stöcker, R.K. Sukumaran, eds. *Recent Advances in Thermo-Chemical Conversion of Biomass*. Boston: Elsevier. pp. 269-291.

[3] Dimitriadis A. and S. Bezergianni. 2017. Hydrothermal liquefaction of various biomass and waste feedstocks for biocrude production. A state of the art review. *Renewable and Sustainable Energy Reviews* 68: 113-125.

[4] Kruse A. and N. Dahmen. 2015. Water – A magic solvent for biomass conversion. *The Journal of Supercritical Fluids* 96: 36-45.

[5] Weingärtner H. and E.U. Franck. 2005. Supercritical Water as a Solvent. *Angewandte Chemie International Edition* 44(18): 2672-2692.

[6] Watanabe M., Aizawa Y., Iida T., Aida T.M., Levy C., Sue K. and Inomata H., 2005. Glucose reactions with acid and base catalysts in hot compressed water at 473K. *Carbohydrate Research* 340(12): 1925-1930.

[7] Shamsul N.S., Kamarudin S.K. and Rahman N.A., 2017. Conversion of bio-oil to bio gasoline via pyrolysis and hydrothermal: A review. *Renewable and Sustainable Energy Reviews* 80: 538-549.

[8] Reißmann D., Thrän D. and Bezama A., 2018. Hydrothermal processes as treatment paths for biogenic residues in Germany: A review of the technology, sustainability and legal aspects. *Journal of Cleaner Production* 172: 239-252.

[9] Mathanker A., Pudasainee D., Kumar A. and Gupta R., 2020. Hydrothermal liquefaction of lignocellulosic biomass feedstock to produce biofuels: Parametric study and products characterization. *Fuel* 271: 117534.

[10] Wu X.-F., Zhang J.-J., Li M.-F., Bian J. and Peng F., 2019. Catalytic hydrothermal liquefaction of eucalyptus to prepare bio-oils and product properties. *Energy Conversion and Management* 199: 111955.

[11] Wu X.-F., Zhou Q., Li M.-F., Li S.-X., Bian J. and Peng F., 2018. Conversion of poplar into bio-oil via subcritical hydrothermal liquefaction: Structure and antioxidant capacity. *Bioresource Technology* 270: 216-222.

[12] Lee J.H., Hwang H. and Choi J.W., 2018. Effects of transition metals on hydrothermal liquefaction

of empty fruit bunches (EFB) for conversion to biofuel and valuable chemicals. *Energy* 162: 1-9.

[13] Malins K., 2017. Production of bio-oil via hydrothermal liquefaction of birch sawdust. *Energy Conversion and Management* 144: 243-251.

[14] Zhu Z., Si B., Lu J., Watson J., Zhang Y. and Liu Z., 2017. Elemental migration and characterization of products during hydrothermal liquefaction of cornstalk. *Bioresource Technology* 243(Supplement C): 9-16.

[15] Zhu Z., Toor S.S., Rosendahl L., Yu D. and Chen G., 2015. Influence of alkali catalyst on product yield and properties via hydrothermal liquefaction of barley straw. *Energy* 80: 284-292.

[16] OAE, 2019. Agricultural Production Data. *Office of Agricultural Economics* [On-line serial], Retrieved September 30, 2020 from the World Wide Web: http://www.oae.go.th/view/1/%E0%B8%82%E0%B9%89%E0%B8%AD%E0%B8%A1%E0%B8%B9%E0%B8%A5%E0%B8%81%E0%B8%B2%E0%B8%A3%E0%B8%9C%E0%B8%A5%E0%B8%B4%E0%B8%95%E0%B8%AA%E0%B8%B4%E0%B8%99%E0%B8%84%E0%B9%89%E0%B8%B2%E0%B9%80%E0%B8%81%E0%B8%A9%E0%B8%95%E0%B8%A3/TH-TH

[17] DEDE, 2013. Biomass potential in Thailand. *Department of Alternative Energy Development and Efficiency* [On-line serial], Retrieved September 30, 2020 from the World Wide Web: http://biomass.dede.go.th/biomass_web/index.html

[18] Pattiya A., Titiloye J.O. and Bridgwater A.V., 2008. Fast pyrolysis of cassava rhizome in the presence of catalysts. *Journal of Analytical and Applied Pyrolysis* 81(1): 72-79.

[19] Meesukanun K. and C. Satirapipathkul. 2014. Production of Acetone-Butanol-Ethanol from Cassava Rhizome Hydrolysate by Clostridium Saccharobutylicum BAA 117. *Chemical Engineering Transactions* 37: 421-426.

[20] Nakason K., Panyapinyopol B., Kanokkantapong V., Viriya-empikul N., Kraithong W. and Pavasant, P., 2018. Characteristics of hydrochar and liquid fraction from hydrothermal carbonization of cassava rhizome. *Journal of the Energy Institute* 91(2): 184-193.

[21] Sluiter A., Hames B., Ruiz R., Scarlata C., Sluiter J. and Templeton D., 2005. *Determination of ash in biomass (NREL/TP-510-42622)*. The US national renewable energy laboratory technical report.

[22] ASTM. 2010. Standard Test Methods for Proximate Analysis of Coal and Coke by Macro Thermogravimetric Analysis. Method D7582-10. ASTM International, Pennsylvania.

[23] ASTM.. 2010. Standard Test Methods for Proximate Analysis of Coal and Coke by Macro Thermogravimetric Analysis. Method D2974-87. ASTM International, Pennsylvania.

[24] Channiwala S.A. and P.P Parikh. 2002. A unified correlation for estimating HHV of solid, liquid and gaseous fuels. *Fuel* 81(8): 1051-1063.

[25] Yang C., Wang S., Ren M., Li Y. and Song W., 2019. Hydrothermal Liquefaction of an Animal Carcass for Biocrude Oil. *Energy & Fuels* 33(11): 11302-11309.

[26] Jadhav A., Ahmed I., Baloch A.G., Jadhav H., Nizamuddin S., Siddiqui M.T.H., Baloch H.A., Qureshi S.S. and Mubarak N.M., 2019. Utilization of oil palm fronds for bio-oil and bio-char production using hydrothermal liquefaction technology. *Biomass Conversion and Biorefinery*.

[27] Zhang S., Zhou S., Yang X., Xi W., Zheng K., Chu C., Ju M. and Liu L., 2020. Effect of operating parameters on hydrothermal liquefaction of corn straw and its life cycle assessment. *Environmental Science and Pollution Research* 27(6): 6362-6374.

[28] Yang L., Nazari L., Yuan Z., Corscadden K., Xu C. and He Q., 2016. Hydrothermal liquefaction of spent coffee grounds in water medium for bio-oil production. *Biomass and Bioenergy* 86: 191-198.

[29] Stauffer E., Dolan J.A., and Newman R., 2008. Chapter 7 - Flammable and Combustible Liquids. In Stauffer E., Dolan J.A., and Newman R, eds. *Fire Debris Analysis*. Burlington: Academic Press, pp. 199-233.

[30] Nakason K., Panyapinyopol B., Kanokkantapong V., Viriya-empikul N., Kraithong W. and Pavasant P., 2017. Hydrothermal Carbonization of Oil Palm Pressed Fiber: Effect of Reaction Parameters on Product Characteristics. *International energy journal* 17(2): 47-56.

[31] Wang W., Xu Y., Wang X., Zhang B., Tian W. and Zhang J., 2018. Hydrothermal liquefaction of microalgae over transition metal supported TiO_2 catalyst. *Bioresource Technology* 250: 474-480.

[32] Lazzari E., Schena T., Marcelo M.C.A., Primaz C.T., Silva A.N., Ferrão M.F., Bjerk T. and Caramão E.B., 2018. Classification of biomass through their pyrolytic bio-oil composition using FTIR and PCA analysis. *Industrial Crops and Products* 111: 856-864.

[33] Álvarez-Murillo A., Román S., Ledesma B. and Sabio E., 2015. Study of variables in energy densification of olive stone by hydrothermal carbonization. *Journal of Analytical and Applied Pyrolysis* 113: 307-314.

[34] Zhang L., Li C.J., Zhou D., Zhang S.C. and Chen J.M., 2013. Hydrothermal Liquefaction of Water Hyacinth: Product Distribution and Identification. *Energy Sources, Part A: Recovery, Utilization, and Environmental Effects* 35(14): 1349-1357.

[35] Zhu Z., Toor S.S., Rosendahl L. and Chen G., 2014. Analysis of product distribution and characteristics in hydrothermal liquefaction of barley straw in subcritical and supercritical water. *Environmental Progress & Sustainable Energy* 33(3): 737-743.

[36] Kang S., Li X., Fan J. and Chang J., 2011. Classified Separation of Lignin Hydrothermal

Liquefied Products. *Industrial & Engineering Chemistry Research* 50(19): 11288-11296.

[37] Chen J., 2018. Bio-oil production from hydrothermal liquefaction of Pteris vittata L.: Effects of operating temperatures and energy recovery. *Bioresource Technology* 265: 320-327

APPENDIX

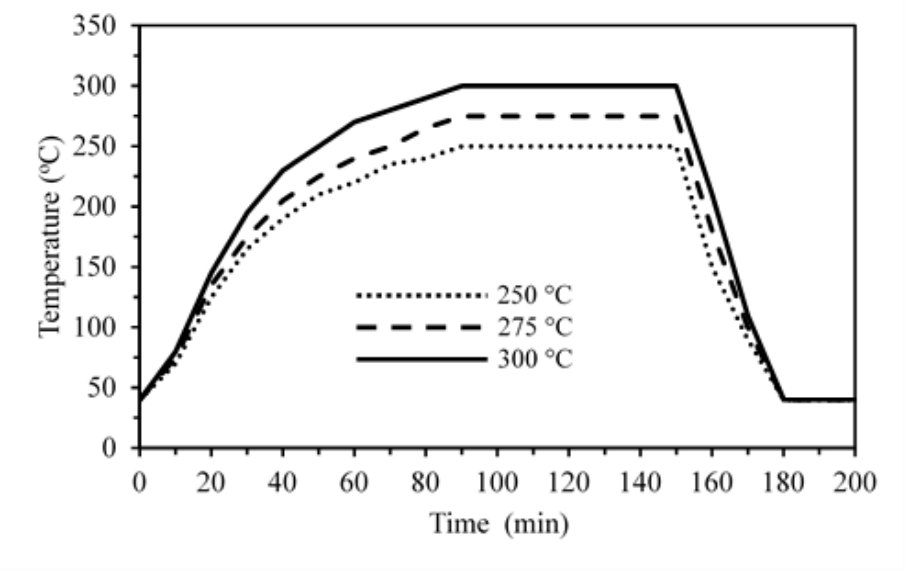

Fig. A1. Temperature profiles in the reactor.

Table A1. Product yield (wt.%) from HTL of CR at 250 – 300°C for 15 – 60 min.

HTL samples	Biocrude oil (BO)	Hydrochar (HC)	Gas and other products	BO:HC ratio
250-15	24.90	37.30	37.80	0.67
250-30	24.40	36.80	38.80	0.66
250-60	22.90	36.90	40.20	0.62
275-15	31.00	33.30	35.71	0.94
275-30	28.60	31.70	39.70	0.90
275-60	28.30	33.70	38.01	0.84
300-15	27.30	29.30	43.41	0.93
300-30	25.10	29.50	45.41	0.85
300-60	25.00	28.80	46.21	0.87

Table A2. The GC-MS analysis of BO.

RT (min)	Compound	Formula	Molecular weight	% area		
				250°C	275°C	300°C
Ketone and Aldehyde				64.16	48.40	47.29
4.51	3-Hexen-2-one (CAS)	$C_6H_{10}O$	98.07	1.80	–	1.68
5.38	Furfural	$C_5H_4O_2$	96.02	15.21	–	–
7.35	2-Cyclopenten-1-one, 2-methyl-	C_6H_8O	96.06	1.19	5.25	5.32
7.41	2-ACETYL FURAN	$C_6H_6O_2$	110.04	4.19	7.55	2.45
8.51	3,6-dioxo-1-methyl-8-isopropyl-tricyclo[6.2.2.0(2,7)]dodec-4,9-diene	$C_{16}H_{20}O_2$	244.15	15.66	7.26	–
8.70	2-Cyclopenten-1-one, 3-methyl- (CAS)	C_6H_8O	96.06	2.09	5.20	5.97
9.74	2-Cyclopenten-1-one, 2-hydroxy-3-methyl- (CAS)	$C_6H_8O_2$	112.05	3.20	–	–
9.76	2,5-Furandione, 3-(1,1-dimethylethyl)-	$C_8H_{10}O_3$	154.06	–	1.05	1.43
9.95	5-Hydroxy-2-heptanone	$C_7H_{14}O_2$	130.10	–	–	4.10

10.01	2-Cyclopenten-1-one, 2,3-dimethyl-	$C_7H_{10}O$	110.07	2.91	3.87	2.84
10.32	2-Cyclohexen-1-one, 3-methyl-	$C_7H_{10}O$	110.07	2.15	3.39	1.04
10.40	2-Cyclopenten-1-one, 3,4,4-trimethyl-	$C_8H_{12}O$	124.09	–	–	1.13
10.64	2-Cyclopenten-1-one, 3-ethyl-	$C_7H_{10}O$	110.07	–	–	1.92
11.03	5-Ethyl-2-furaldehyde	$C_7H_8O_2$	124.05	–	–	1.31
						…cont'd
11.08	2-Cyclopenten-1-one, 3-(1-methylethyl)-	$C_8H_{12}O$	124.09	–	–	1.39
11.11	1H-Inden-1-one, 2,3-dihydro- (CAS)	C_9H_8O	132.06	1.51	3.53	2.11
11.72	3-Hexen-2-one, 3,4-dimethyl-, (E)-	$C_8H_{14}O$	126.10	–	–	0.91
12.38	2-Acetonylcyclopentanone	$C_8H_{12}O_2$	140.08	–	–	0.56
12.40	3-Buten-2-one, 4-(2-furanyl)-	$C_8H_8O_2$	136.05	1.48	–	–
12.98	5-Hydroxymethylfurfural	$C_6H_6O_3$	126.03	6.77		
13.56	(2-Methyl-cyclohex-2-enylidene)-acetaldehyde	$C_9H_{12}O$	136.09	–	–	0.95
13.76	2,5-Diacetylfuran	$C_8H_8O_3$	152.05	0.95	1.61	3.69
14.14	H-Inden-2-one, 1,4,5,6,7,7a-hexahydro-7a-methyl-, (S)-	$C_{10}H_{14}O$	150.10	0.76	–	–
14.18	anti-(2SR,3SR)-3-Hydroxy-2,2,4-trimethylthiaolane	$C_7H_{14}OS$	146.08	2.04	3.65	–
14.45	2-Cyclohexen-1-one, 5-methyl-2-(1-methylethyl)-	$C_{10}H_{16}O$	152.12	0.47	3.76	1.79
14.98	4,5,6,7,8,9-hexahydrocycloocta[c]furan-1(3H)-one	$C_{10}H_{14}O_2$	166.10	–	–	2.08
15.61	Benzaldehyde, 2,4,6-trimethyl-	$C_{10}H_{12}O$	148.09	–	–	1.19
16.06	2-Cyclopenten-1-one, 3-methyl-2-(2,4-pentadienyl)-, (Z)-	$C_{11}H_{14}O$	162.10	1.77	2.29	1.44
16.67	Benzaldehyde, 2,3,4,5-tetramethyl-	$C_{11}H_{14}O$	162.10	–	–	1.34
18.78	Nootkaton-11,12-epoxide	$C_{15}H_{22}O_2$	234.16	–	–	0.65
Phenols				21.96	29.05	30.4
8.85	Phenol (CAS)	C_6H_6O	94.04	0.90	–	1.78
10.20	Phenol, 3-methyl-	C_7H_8O	108.06	–	–	0.96
10.56	Phenol, 4-methyl- (CAS)	C_7H_8O	108.06	0.61	–	1.58
10.81	Phenol, 2-methoxy- (CAS)	$C_7H_8O_2$	124.05	6.38	10.20	13.32
12.48	Creosol	$C_8H_{10}O_2$	138.07	–	–	3.04
14.76	Phenol, 2,6-dimethoxy- (CAS)	$C_8H_{10}O_3$	154.06	3.47	5.31	3.24
16.66	dimethyltbenzo[b]hiophene	$C_{10}H_{10}S$	162.05	2.01	–	–
16.80	2-tert-Butyl-4-isopropyl-5-methylphenol	$C_{14}H_{22}O$	206.17	8.59	13.54	6.48
Alcohols				2.15	–	5.49
9.15	Cyclohexanol, 2,3-dimethyl-	$C_8H_{16}O$	128.12	–	–	1.93
9.91	(Z)-2,6,6-Trimethyl-α-(1-propenyl)-2-cyclohexane-1-methanol	$C_{13}H_{22}O$	194.17	1.37	–	0.76
10.62	ORCINOL	$C_7H_8O_2$	124.05	0.78	–	–
11.12	3-Phenylprop-2-yn-1-ol	C_9H_8O	132.06	–	–	1.30
11.23	2H-Indeno[1,2-b]oxirene, octahydro-, (1aα,1bβ,5aα,6aα)-	$C_9H_{14}O$	138.10	–	–	1.50
Hydrocarbons				11.07	20.61	12.96
9.16	Decane	$C_{10}H_{22}$	142.17	0.92	2.35	–
11.55	Cyclohexane, (1-methylethylidene)-	C_9H_{16}	124.13	1.24	–	0.84
12.55	Dodecane (CAS)	$C_{12}H_{26}$	170.20	2.49	5.50	2.50
15.35	Tetradecane	$C_{14}H_{30}$	198.234	3.24	7.00	4.65
17.81	Hexadecane	$C_{16}H_{34}$	226.27	2.31	3.94	2.72
20.02	Octadecane (CAS)	$C_{18}H_{38}$	254.30	0.87	1.82	1.47

22.03	Dotriacontane (CAS)	$C_{32}H_{66}$	450.52	–	–	0.78
Esters				0.66	1.94	–
2.41	Propanoic acid, ethyl ester (CAS)	$C_5H_{10}O_2$	102.07	0.66	1.94	–
Organic acids				–	–	2.90
11.78	α-Campholonic acid	$C_{10}H_{16}O_2$	168.12	–	–	1.26
						…cont'd
15.25	Hydrocinnamic acid, o-[(1,2,3,4-tetrahydro-2-naphthyl)methyl]-	$C_{20}H_{22}O_2$	294.16	–	–	1.64
Amines				–	–	0.96
16.01	Benzenamine, 2-methoxy-5-nitro- (CAS)	$C_7H_8N_2O_3$	168.05	–	–	0.96
	Total			100	100	100